Research Article

Journal of MASS SPECTROMETRY

Received: 8 June 2011 Revised: 9 September 2011 Accepted: 14 November 2011 Published online in Wiley Online Library

(wileyonlinelibrary.com) DOI 10.1002/jms.2028

Cyclochiral resorcin[4]arenes as effective enantioselectors in the gas phase

Caterina Fraschetti,[a,b]* Matthias C. Letzel,[a] Marlene Paletta,[a] Jochen Mattay,[a] Maurizio Speranza,[b] Antonello Filippi,[b] Massimiliano Aschi[c] and Alexander B. Rozhenko[a,d]

The effect of cyclochirality of *rccc*-2,8,14,20-tetra-*n*-decyl-4,10,16,22-tetra-*O*-methylresorcin[4]arene (C) on the enantiodiscrimination of a number of chiral bidentate and tridentate aromatic and aliphatic biomolecules (G) has been investigated by nano-electrospray ionization (nano-ESI)-Fourier transform ion cyclotron resonance mass spectrometry. The experimental approach is based on the formation of diastereomeric proton-bound $[C{\cdot}H{\cdot}G]^+$ complexes by nano-ESI of solutions containing an equimolar amount of *quasi*-enantiomers (C) together with the chiral guest (G) and the subsequent measurement of the rate of the G substitution by the attack of several achiral and chiral amines. In general, the heterochiral complexes react faster than the homochiral ones, except when G is an aminoalcoholic neurotransmitter whose complexes, beyond that, exhibit the highest enantioselectivity. The kinetic results were further supported by both collision-induced dissociation experiments on some of the relevant $[C_2{\cdot}H{\cdot}G]^+$ three-body species and Density functional theory (DFT) calculations performed on the most selective systems. Copyright © 2012 John Wiley & Sons, Ltd.

Supporting information may be found in the online version of this article.

Keywords: cyclochirality; resorc[4]arene; enantiodiscrimination; gas phase; FT-ICR; inherent chirality; ligand exchange; supramolecular complex

INTRODUCTION

One of the most important goals of the supramolecular chemistry is the construction of artificial receptors, which can mimic enzyme activity and selectivity, and are applicable to asymmetric syntheses. The noncovalent interactions established between chiral host molecules, for example, proteins, with a variety of guests, as well as the origin of diastereoselection in the nucleophilic capture by chiral cation, have been intensively investigated in the gaseous phase, where solvation effect and ion pairing do not interfere.[1–6] In general, the gas-phase studies of diastereomeric complexes provide an efficient probe to evaluate the intrinsic factors governing enantiorecognition processes.[7] Chiral resorcin[4]arenes are commonly recognized as instances of potential receptors successfully employed in enantiorecognition and catalysis.[8–10] Regarding resorcin[4]arenes, chirality can be due to (1) the presence of stereogenic centers in their side chains, and (2) the spatial arrangement of achiral subunits forming a structurally chiral macrocyclic scaffold.

The concepts of 'cyclochirality' and 'inherent chirality' apply to the latter case. 'Cyclochirality' is defined as molecular asymmetry due to the sense of direction of the rings in a XXXX system composed by the same building blocks, chemically locked as in the case of rotaxanes[11] or noncovalently locked by hydrogen bonds[12], whereas the 'inherent chirality' is referred to as a covalently blocked curvature of a XXYZ or WXYZ system.[13] To date, the recognition capability of gaseous resorcin[4]arenes has been kinetically explored using predominantly chiral macrocycles of type 1).[14–22] A first study on the complexation behavior of a cyclochiral resorcinarene towards several chiral quaternary ammonium ions has been investigated by us using the ESI-mass spectrometry methodology.[23] To shed more light on the intrinsic factors governing enantiodiscrimination by cyclochiral receptors, we generated proton-bound adducts between resorcinarenes **C** (Chart 1) and several chiral bidentate or tridentate biomolecules (**G**, Table 1), and their reactivity towards some primary amines (Chart 1; **B**: CH_3CHWNH_2 with W = H, CH_3, C_2H_5) has been measured in the gaseous phase. The cyclochirality of the macrocycles of Chart 1 is due to the presence of four methoxy and four hydroxy groups on the aromatic scaffold, which are arranged either clockwise or counterclockwise. Following the stereochemical nomenclature for compounds of axial symmetry, we denote the two cyclochiral enantiomers of Chart 1 as (*M,R*)-**C** and (*P,S*)-**C** (**C**$_{M,R}$ and **C**$_{P,S}$ in Chart 1). *M* and *P* notations are referred to the axial chirality of the compound, whereas *R* and *S* describe the inter-ring configuration centers.[24]

* *Correspondence to: Caterina Fraschetti, Department of Chemistry Bielefeld University, P.O. Box 100131, 33501, Bielefeld, Germany. E-mail: caterina.fraschetti@uniroma1.it*

a *Department of Chemistry Bielefeld University, P.O. Box 100131, 33501, Bielefeld, Germany*

b *Department of Chemistry and Technologies of Drug, Sapienza-University of Rome, Piazzale Aldo Moro, 5, 00185, Rome, Italy*

c *Department of Chemistry, L'Aquila University, Via Vetoio s.n.c. Coppito, L'Aquila, Italy*

d *Institute of Organic Chemistry of the National Academy of Sciences of Ukraine, Murmans'ka str. 5, 02094 Kyiv, Ukraine*

Journal of MASS SPECTROMETRY

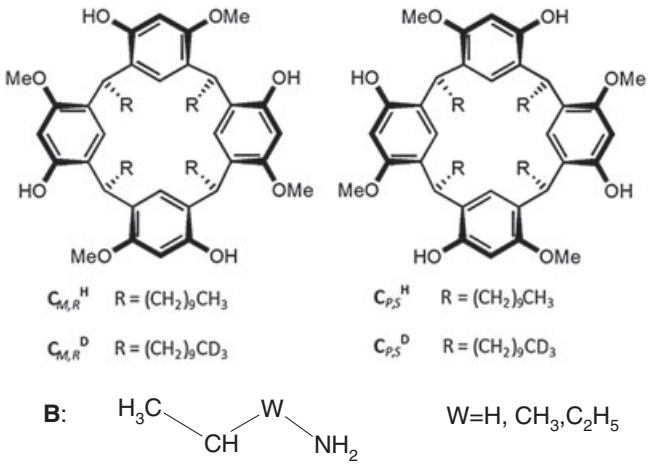

Chart 1. Cyclochiral Resorcinarenes (C) and neutral amine (B) used in the gas-phase investigaton.

It is well known that naked cyclochiral macrocycles may have either a C_4 (*crown*) or a C_2 (*boat*) symmetry and that resorcinarene **C** is a C_4-symmetrical macrocycle[25] with a chiral concave surface suitable for noncovalent interactions with selected polar guests. It should be noted that the resorcinarene conformation may be somewhat influenced in solution by the polarity of the medium. The *crown*⇄*boat* conformational equilibrium is shifted to the right in going from aprotic to protic solvent because the intramolecular hydrogen bond network stabilizing the C_4 symmetry is partially disrupted by intermolecular hydrogen bonding with the protic molecules of the solvent.[26] The orientation of guests on the upper aromatic cavity of **C** should be further favored by the presence of a second but apolar cavity on the opposite side formed by the very long aliphatic chains. Their terminal-CX_3 methyl groups (X = H, D) allow the use of *quasi*-racemic mixtures of the cyclochiral hosts, thus enabling the simultaneous measurements of the reactivity of the corresponding *quasi*-diastereomeric complexes, (e.g., $[\mathbf{C}_{P,S}^{H}\cdot H\cdot \mathbf{G}]^+$ and $[\mathbf{C}_{M,R}^{D}\cdot H\cdot \mathbf{G}]^+$) (Eqn (1)).[27]

$$\left[\mathbf{C}_{P,S}^{H}\cdot H\cdot \mathbf{G}\right]^+ + \mathbf{B} \rightarrow \left[\mathbf{C}_{P,S}^{H}\cdot H\cdot \mathbf{B}\right]^+ + \mathbf{G} \qquad (1a)$$

$$\left[\mathbf{C}_{M,R}^{D}\cdot H\cdot \mathbf{G}\right]^+ + \mathbf{B} \rightarrow \left[\mathbf{C}_{M,R}^{D}\cdot H\cdot \mathbf{B}\right]^+ + \mathbf{G} \qquad (1b)$$

EXPERIMENTAL SECTION

Materials

The $\mathbf{C}_{P,S}^{D}/\mathbf{C}_{M,R}^{D}$ racemate was synthesized as reported in Scheme 1 and purified by recrystallization.[28–32] The deuteration level of the racemate was measured by means of ESI-mass spectrometry technique as exceeding 99%. The $\mathbf{C}_{P,S}^{D}/\mathbf{C}_{M,R}^{D}$ racemate, as well as the $\mathbf{C}_{P,S}^{H}/\mathbf{C}_{M,R}^{H}$ one, were resolved by reaction with freshly prepared (*S*)-(+)-10-camphorsulfonyl chloride, K_2CO_3, and dimethylamphetamine in a THF/acetonitril mixture (2:3 v:v) to yield the functionalized diastereomers, subsequently separated by silica gel high-performance liquid chromatography. The diastereomeric excess was determined by means of NMR spectroscopy as >99%. The monocamphorsulfonates diastereomers were then hydrolyzed under alkaline conditions into the enantiomerically pure resorcin[4]arenes (−)-$\mathbf{C}_{M,R}^{H}$ and (+)-$\mathbf{C}_{P,S}^{H}$ and their deuterated *quasi*-enantiomeric counterparts (−)-$\mathbf{C}_{M,R}^{D}$ and (+)-$\mathbf{C}_{P,S}^{D}$. The absolute configuration of the cyclochiral resorcinarenes is known from earlier studies by Heaney *et al.*[24] The CD and NMR spectroscopic details are described in Supporting Information. All the other employed substances are commercially available.

ESI-FT-ICR experiments

The experiments were performed at room temperature in an APEX III 7.0 Tesla Fourier transform ion cyclotron resonance (FT-ICR) mass spectrometer (Bruker Daltonic GmbH, Bremen) fitted with a nano-ESI source (Apollo) and a resonance cell (infinity cell). The starting $CH_3OH/CHCl_3$ (10:1) solutions contained the cyclochiral hosts $\mathbf{C}_{P,S}^{H}$ (1×10^{-5} M), $\mathbf{C}_{M,R}^{D}$ (1×10^{-5} M) and the selected guest **G** (6×10^{-5} M). The resulting ions were transferred into the resonance cell by using an accumulation hexapole and a system of potentials and lenses. Finally, the ions were cooled by collisions with Argon, pulsed into the cell through a magnetic valve. The mass spectra of the ESI solutions are characterized by the almost exclusive presence of the intense signals corresponding to the proton-bound complexes $[\mathbf{C}\cdot H\cdot \mathbf{G}]^+$. These noncovalently charged aggregates were isolated by broad-band ejection of the accompanying ions and were allowed to react with a neutral gas **B** (**B** = $C_2H_5NH_2$, *iso*-$C_3H_7NH_2$, *(R)* or *(S)-sec*-$C_4H_9NH_2$), present in the cell at controlled pressure (from 2.0×10^{-9} to 4.5×10^{-8} mbar, depending upon their reactivity). Comparison of the kinetic results obtained with the *quasi*-diasteromeric $[\mathbf{C}_{P,S}^{H}\cdot H\cdot \mathbf{G}]^+/[\mathbf{C}_{M,R}^{D}\cdot H\cdot \mathbf{G}]^+$ mixture with the reversed combination $[\mathbf{C}_{P,S}^{D}\cdot H\cdot \mathbf{G}]^+/[\mathbf{C}_{M,R}^{H}\cdot H\cdot \mathbf{G}]^+$ safely excludes any isotope effect on the kinetics of Eqn (1). Each kinetics has been repeated not less than three times to evaluate the experimental error.

ESI-CID experiments

Collision-induced dissociation (CID) experiments were performed on a Micromass Quattro LCZ (Waters-Micromass, Manchester, UK) equipped with a nano-electrospray ionization (nano-ESI) source. Operating conditions of the nano-ESI source are as follows: capillary voltage = +1.29 kV, cone = 41 V, collision energy = 14.2 eV, and source block temperature = 60 °C. Methanolic solutions were introduced via a nanospray needle. CID experiments were performed in the following way: after isolation in the first quadrupole, the precursor ion was transferred to the collision chamber, where it was fragmented by collisions with Ar. The resulting ions were analyzed in the second quadrupole. The nominal pressure of argon in the collision chamber was 8.0×10^{-4} mbar. The relative abundance of fragments results from the area of peaks of the spectra acquired in profile mode. Multiple scans were accumulated until a satisfying s/n was achieved.

Computational details

For more rapid calculations, the decamethylene lateral chains were replaced by methyl groups and the obtained adducts were optimized using the TURBOMOLE suit program[33] (version 6.02). For every diastereoisomer, 8–10 different structures were fully optimized, and their total energies were compared. Noteworthy, the adduct structures with lowest total energies are indeed stabilized by a H–O, H–N, and H–π hydrogen bonds network. Such approach does not ensure finding true global minima but provides several indicative conformations, which possess lowest total energy values and hence should strongly contribute into the distribution of conformational isomers. The BP86 DFT

Table 1. Investigated Guests, **G**

Free AA	R	R′		Aminoalcohol		
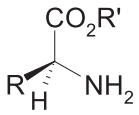						
L-phenylalanine	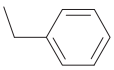	H	A_1	L-tyrosinol	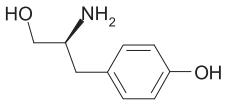	N_1
3,4-dihydroxy-L-phenylalanine	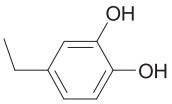	H	A_2	(1R,2R)-2-amino-1-phenyl-1,3-propandiol	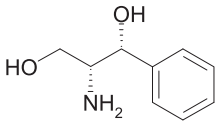	N_2
L-tryptophan	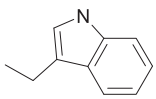	H	A_3	L-epinephrine	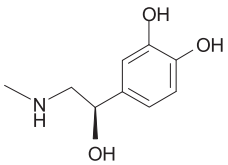	N_3
5-hydroxy-L-tryptophan	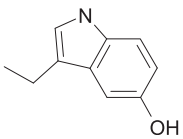	H	A_4	L-norepinephrine	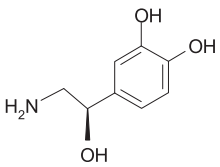	N_4
L-tyrosine	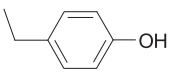	H	A_5			
AA ester						
L-phenylalanine ethyl ester	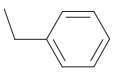	C_2H_5	E_1			
L-tyrosine methyl ester	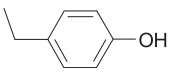	CH_3	E_2			

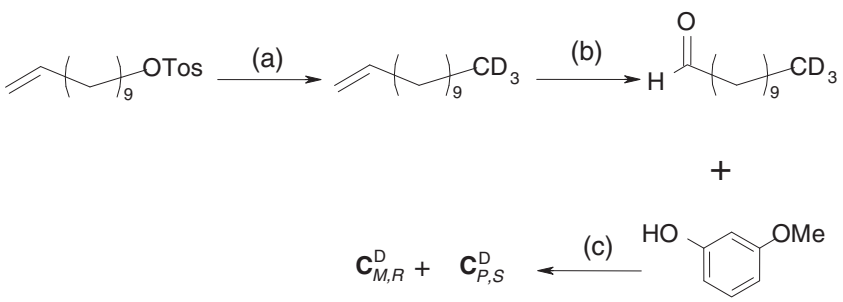

Scheme 1. Synthesis of the labeled quasi-racemate of $\mathbf{C}_{M,R}^{\mathbf{D}}$ and $\mathbf{C}_{P,S}^{\mathrm{D}}$. (a) 1.9 eq. d_3-MeMgI (1.0 M in Et_2O), 3 mol% $CuCl_2$ and 12 mol% 1-phenyl propyne in THF, 12 h (95% isolated yield), (b) 3.6 mol% $RuCl_3$ $(H_2O)_3$, 2.5 eq. $NaIO_4$, MeCN/H_2O (92:8 v:v), 16 h (62% isolated yield), (c) 2 eq. $BF_3{\cdot}OEt_2$ in dichloromethane, −10 °C, 1 h (56% isolated yield).

Journal of MASS SPECTROMETRY

functional[34,35] was used in combination with the standard SV(P) basis sets. The *Resolution of the Identity* algorithm[36] implemented in the TURBOMOLE packet[37] was employed for the high calculation efficiency. Every optimized structure was modified to increase the number of hydrogen bonds in the adduct and was then re-optimized. The procedure was repeated until no more lowering total energy was observed. The most favored structures were re-optimized using the same functional and the TZVP extended basis sets (TZV basis sets[38] of triple-zeta quality plus one p-function set for hydrogen, TZV plus one d-function set for all the other atoms). Finally, to take into account the electronic dispersion effects, we re-optimized the most favored structures using Grimme's B97-D functional[39,40] and the above-mentioned TZVP basis sets. The vibrational frequencies were calculated at the RI-BP86/TZVP and RI-B97-D/TZVP levels of theory, deriving gradients numerically.[41] The relative energy (ΔE) magnitudes were computed using zero-point energy (ZPE)-corrected total energy values, whereas the relative free Gibbs energy magnitudes (ΔG) were obtained from the same total energy values corrected by chemical potential (CP) correction values (Table S5 in Supporting Information). The default scaling factor (0.9914) was used for the ZPE and CP correction values. All the thermodynamic parameters were computed using *freeh* routine for T = 298.15 K and P = 0.1 MPa. The calculated structures were presented using the visual molecular dynamics program set.[42]

Kinetic results

According to ^{1}H-NMR evidence, competitive solvation prevents the formation of neutral [**C**·**G**] aggregates (in $CDCl_3$ or $CDCl_3$/CD_3OD solutions; Supporting Information). Thus, the proton-bound $[\mathbf{C}\cdot\mathrm{H}\cdot\mathbf{G}]^+$ complexes are essentially generated in the evaporating nano-ESI nanodroplets. The kinetic profile of reactions 1 was analyzed by plotting the $\log([\mathbf{C}\cdot\mathrm{H}\cdot\mathbf{G}]_t^+/[\mathbf{C}\cdot\mathrm{H}\cdot\mathbf{G}]_0^+)$ *versus* the reaction time, where $[\mathbf{C}\cdot\mathrm{H}\cdot\mathbf{G}]_t^+$ is the precursor abundance at time *t* and $[\mathbf{C}\cdot\mathrm{H}\cdot\mathbf{G}]_0^+$ is the sum of the $[\mathbf{C}\cdot\mathrm{H}\cdot\mathbf{G}]_t^+$ and the $[\mathbf{C}\cdot\mathrm{H}\cdot\mathbf{B}]^+$ complexes. All the kinetic plots exhibit a mono-exponential decay with an excellent correlation ($0.998 < r^2 < 0.999$), which could suggest the predominance of a single $[\mathbf{C}\cdot\mathrm{H}\cdot\mathbf{G}]^+$ structure or the coexistence of structures that react with undistinguishable *k*. The slopes of the mono-exponential kinetic plots provide a measure of the corresponding pseudo-first order rate constants (*k*′) of Eqn (1). The relevant second-order constants (*k*) are calculated as $k = k'/[\mathbf{B}]$. Comparison of *k* with the corresponding thermal capture collision rate k_{cap} provides an estimate of the reaction efficiency (eff = 100 k/k_{cap}; Supporting Information).[43] The effect of the resorcinarene's cyclochirality is described by the ratio $\rho = k_{homo}/k_{hetero}$, where k_{homo} refers to the rate constant measured when the host and the guest have the same chirality and k_{hetero} to that measured when the host and the guest have opposite nominal configuration. The obtained enantioselectivity ratios $\rho = k_{homo}/k_{hetero}$ are summarized in Table 2 (the individual rate constants are reported in Tables S1–S3). It should be noted that the enantioselectivity of the competing reactions 1 increases as the ρ values diverges from unity. Control experiments have been performed by employing the glycine ethyl ester as an achiral guest, where no appreciable deviation of ρ from unity has been obtained ($[\mathbf{C}_{P,S}{}^{\mathbf{H}}\cdot\mathrm{H}\cdot\mathbf{G}]^+/[\mathbf{C}_{M,R}{}^{\mathbf{D}}\cdot\mathrm{H}\cdot\mathrm{G}]^+$ $\rho = 0.98 \pm 0.06$ and $[\mathbf{C}_{P,S}{}^{\mathbf{D}}\cdot\mathrm{H}\cdot\mathbf{G}]^+/[\mathbf{C}_{M,R}{}^{\mathbf{H}}\cdot\mathrm{H}\cdot\mathbf{G}]^+$ $\rho = 1.00 \pm 0.06$). Ligand exchange reactions of $CH_3CH_2NH_2$ on $[\mathbf{C}\cdot\mathrm{H}\cdot\mathbf{G}]^+$ complexes of N_2, N_3, and N_4 do not occur under the used experimental conditions. As shown in Table 2, most of the enantioselectivity values fall at $\rho \leq 1.00$, thus indicating that the heterochiral complexes react faster than the homochiral homologues. The opposite behavior ($\rho > 1.00$) is observed for the $[\mathbf{C}\cdot\mathrm{H}\cdot\mathbf{G}]^+$ complexes with $\mathbf{G} = A_4$, N_2, N_4. In Fig. 1, an instance of representative mass spectra describing the reaction of $[\mathbf{C}\cdot\mathrm{H}\cdot\mathbf{N_2}]^+$ towards *iso*-propylamine has been reported: as the delay time increases, the diastereoisomer precursor ions disappear and the exchanged product is formed with different efficiency, depending on the configuration of **C**. Besides, taking into account that the experimental uncertainty associated with the measured kinetics does not exceed ±10%, the comparison of the $[\mathbf{C}_{P,S}{}^{\mathbf{H}}\cdot\mathrm{H}\cdot\mathbf{G}]^+/[\mathbf{C}_{M,R}{}^{\mathbf{D}}\cdot\mathrm{H}\cdot\mathbf{G}]^+$ and $[\mathbf{C}_{P,S}{}^{\mathbf{D}}\cdot\mathrm{H}\cdot\mathbf{G}]^+/[\mathbf{C}_{M,R}{}^{\mathbf{H}}\cdot\mathrm{H}\cdot\mathbf{G}]^+$ pairs confirms that their reactions 1 are not affected by significant isotope effects, except for $\mathbf{G} = N_1$ with $\mathbf{B} = iso\text{-}C_3H_7NH_2$ (Table S4; KIE = 0.74).[44]

Theoretical results

To explain the origin of the measured enantioselectivity, we performed a theoretical analysis to elucidate the structural features of the $[\mathbf{C}\cdot\mathrm{H}\cdot\mathbf{G}]^+$ noncovalent adducts. In this view, some preliminary aspects should be discussed: (1) the actual location of the proton in the $[\mathbf{C}\cdot\mathrm{H}\cdot\mathbf{G}]^+$ complexes, whether preferentially bound

Table 2. k_{homo}/k_{hetero} measured for reactions of $[\mathbf{C}^{\mathbf{H}}\cdot\mathrm{H}\cdot\mathbf{G}]^+/[\mathbf{C}^{\mathbf{D}}\cdot\mathrm{H}\cdot\mathbf{G}]^+$ complexes with **B**

	W = H	W = CH_3	W = C_2H_5 (*R*)-	W = C_2H_5; (*S*)-
P.A.	210	212.5	214.1	214.1
G		k_{homo}/k_{hetero} (ρ)		
A_1	0.99 ± 0.07		1.10 ± 0.04	1.10 ± 0.08
A_2	0.39 ± 0.01	0.70 ± 0.05	0.93 ± 0.06	0.94 ± 0.04
A_3	0.56 ± 0.02		0.95 ± 0.06	1.08 ± 0.07
A_4		2.03 ± 0.11	1.31 ± 0.08	1.44 ± 0.09
A_5			0.95 ± 0.05	0.99 ± 0.06
E_1	0.53 ± 0.03	0.74 ± 0.03	0.77 ± 0.03	0.82 ± 0.08
E_2		0.80 ± 0.04	0.82 ± 0.04	0.84 ± 0.05
N_1	0.59 ± 0.03	0.47 ± 0.02	0.54 ± 0.03	0.76 ± 0.03
N_2		3.89 ± 0.29	3.94 ± 0.23	2.65 ± 0.38
N_3		0.89 ± 0.04	1.02 ± 0.04	0.78 ± 0.03
N_4		1.51 ± 0.09	1.57 ± 0.09	1.32 ± 0.08

P.A. values are reported in kcal mol^{-1} and have been by taken from a web source.[46]

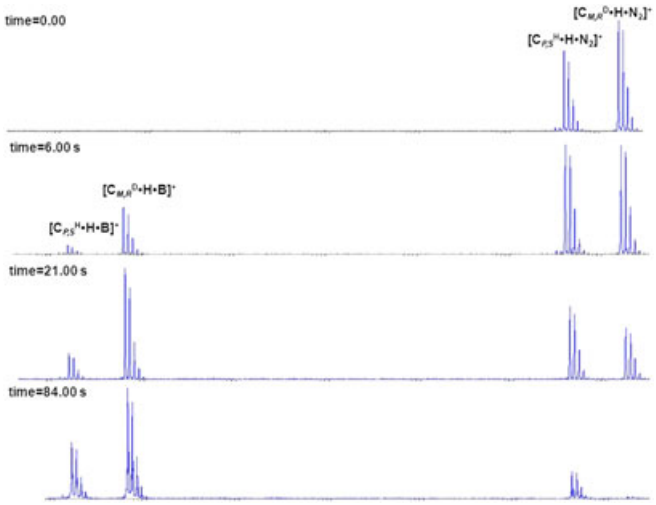

Figure 1. Time dependent mass spectra of the reaction of $[\mathbf{C}\cdot H\cdot N2]^+$ complexes towards *iso*-propylamine.

to the **C** or to the **G** moieties, and (2) the actual location of guest **G** in the proton-bound $[\mathbf{C}\cdot H\cdot\mathbf{G}]^+$ complexes. The optimized structures of adducts of simplified *rccc*-2,8,14,20-tetra-methyl-4,10,16,22-tetra-*O*-methylresorcin[4]arene (**C′**) with the more efficiently enantiorecognized guests (N_1, N_2) are shown in Figs. 2–3. In the most favored structures of the N_1 adducts, the guest is located in the upper chiral rim of the host; meanwhile, its -NH_3^+ charged head is located exactly in the center of the basket, engaged in NH–π multiple interactions. This predicted protonation site is consistent with the ESI-CID experiments on some representative $[\mathbf{C}\cdot H\cdot\mathbf{G}]^+$ complexes, which gave $[H\cdot\mathbf{G}]^+$ as unique fragmentation product, thus pointing to the amino group of the guest as the most basic site within the complexes. The aliphatic OH is engaged in O-H_{guest} –O-CH_{3host} hydrogen bonding, whereas the aromatic hydroxyl group is preferably located outside the cavity. The corresponding couple of diastereoisomeric structures of $[\mathbf{C}\cdot H\cdot N_2]^+$ aggregates is shown in Fig. 3. For the homochiral adduct, the ammonium group is again inside the host cavity, whereas in the heterochiral $[\mathbf{C}\cdot H\cdot N_2]^+$, the ammonium group is shifted towards the corner of the host possessing the crown conformation. In both cases, there is a hydrogen bond network involving two O-H_{guest} –O-CH_{3host} interactions.

DISCUSSION

The effect of the amine configuration ((*R*)-(−)-2-$C_4H_9NH_2 = k_{(R)}$ *vs* (*S*)-(+)-2-$C_4H_9NH_2 = k_{(S)}$) on reactions 1 is inferred from the relevant $\xi = k_{(R)}/k_{(S)}$ ratios reported in Tables S1–S3. The observation that the measured ξ values, in most cases, significantly diverges from unity strongly indicates that the rate-determining step of reaction involves a direct interaction between 2-$C_4H_9NH_2$ and the diastereoisomeric scaffold of the complex. Because the **B**-to-**G** displacement requires a prototropic transfer between the two species, it is concluded that the chiral amine **B** must approach the proton-bound complex *frontside* by developing an effective interaction of the latter with the chiral upper rim of the host before releasing the neutral guest.

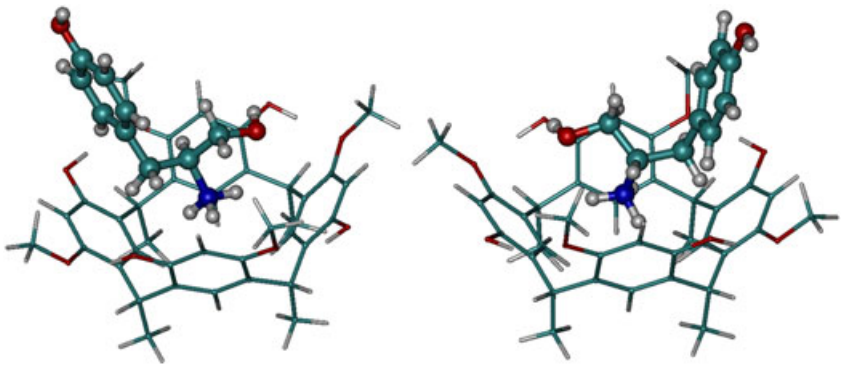

Figure 2. Optimized structures of the diastereomeric heterochiral and homochiral $[\mathbf{C}'\cdot H\cdot N1]^+$ complexes.

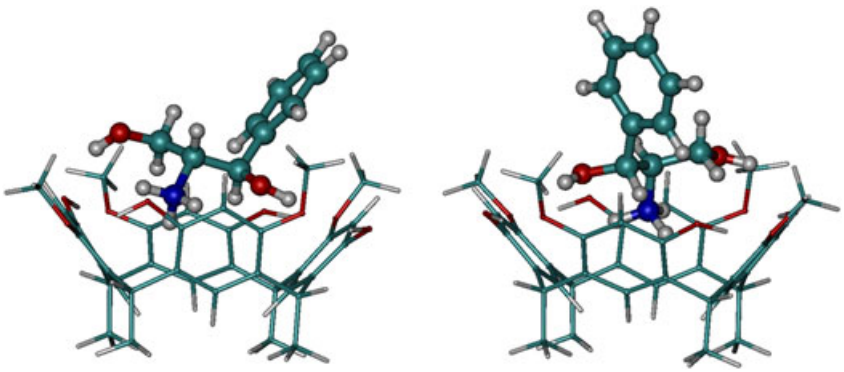

Figure 3. Optimized structures of the diastereomeric heterochiral and homochiral $[\mathbf{C}'\cdot H\cdot N2]^+$ complexes.

Journal of MASS SPECTROMETRY

In principle, the enantioselectivity ρ values of Table 2 may essentially reflect the different stability of diastereomeric $[\mathbf{C}\cdot H\cdot\mathbf{G}]^+$ complexes, coupled with *quasi*-isoenergetic transition structures (thermodynamic enantioselectivity). Alternatively, the measured ρ values are due to different transition structures stability connecting *quasi*-degenerate diastereomeric $[\mathbf{C}\cdot H\cdot\mathbf{G}]^+$ complexes to products (kinetic enantioselectivity). Of course, the experimentally observed kinetic scenario may reflect a combination of these possibilities.

Analysis of Tables S1–S3 reveals that in all cases, the reaction efficiency (*eff*) for a given $[\mathbf{C}\cdot H\cdot\mathbf{G}]^+$ complex increases by increasing the proton affinity of **B** and by decreasing that of the coordinated guest **G** (in the order $N \rightarrow E \rightarrow AA$).[46] Furthermore, in all virtually examined cases, the increase of the **B** proton affinity, which should make the relevant transition structures more similar to the reactant $[\mathbf{C}\cdot H\cdot\mathbf{G}]^+$ structures than to the product $[\mathbf{C}\cdot H\cdot\mathbf{B}]^+$, is accompanied by the tendency of enantioselectivity ρ terms to the unity. On these grounds, it is unlikely that the measured enantioselectivities simply reflect the different stability of diastereomeric $[\mathbf{C}\cdot H\cdot\mathbf{G}]^+$ complexes, but rather they are thought to arise from the different stability of the transition structures on the reaction pathway to products. This conclusion finds an independent support from the relative stability of the diastereomeric $[\mathbf{C}\cdot H\cdot\mathbf{G}]^+$ complexes obtained by collision-induced dissociation (CID) of the $[\mathbf{C}_{M,R}^{\mathbf{X}}\cdot\mathbf{C}_{P,S}^{\mathbf{Y}}\cdot H\cdot\mathbf{G}]^+$ ($\mathbf{G} = N_1$; N_2; X,Y = H,D or D,H) ions. CID of $[\mathbf{C}_{M,R}^{\mathbf{X}}\cdot\mathbf{C}_{P,S}^{\mathbf{Y}}\cdot H\cdot\mathbf{G}]^+$ (X,Y = H,D or D,H) is expected to yield the corresponding $[\mathbf{C}_{M,R}^{\mathbf{X}}\cdot H\cdot\mathbf{G}]^+$ or $[\mathbf{C}_{P,S}^{\mathbf{Y}}\cdot H\cdot\mathbf{G}]^+$ (X,Y = H,D or D,H) fragments after loss of the other host molecule. Although it is well recognized that Cook's method is not particularly suited for large and polydentate systems, wherein collisional dissociation may involve not negligible activation barriers and entropy factors, nevertheless, in this specific case, it can be assumed that the differential $\Delta\Delta S^{\ddagger} = \Delta S^{\ddagger}_{homo} - \Delta S^{\ddagger}_{hetero}$ contributions are negligible, as related to the loss of two enantiomeric forms of the same host. It follows that the relative abundance of the $[\mathbf{C}_{M,R}^{\mathbf{H}}\cdot H\cdot\mathbf{G}]^+$ and $[\mathbf{C}_{P,S}^{\mathbf{D}}\cdot H\cdot\mathbf{G}]^+$ (or $[\mathbf{C}_{M,R}^{\mathbf{D}}\cdot H\cdot\mathbf{G}]^+$ and $[\mathbf{C}_{P,S}^{\mathbf{H}}\cdot H\cdot\mathbf{G}]^+$) fragments from CID of their $[\mathbf{C}_{M,R}^{\mathbf{X}}\cdot\mathbf{C}_{P,S}^{\mathbf{Y}}\cdot H\cdot\mathbf{G}]^+$ precursors can represent a reliable estimate of their relative stability. In this frame, the diastereomeric $[\mathbf{C}_{M,R}^{\mathbf{X}}\cdot H\cdot N_1]^+$ and $[\mathbf{C}_{P,S}^{\mathbf{Y}}\cdot H\cdot N_1]^+$ complexes can be considered as nearly degenerate because of their almost equal abundance from CID of $[\mathbf{C}_{M,R}^{\mathbf{X}}\cdot\mathbf{C}_{P,S}^{\mathbf{Y}}\cdot H\cdot N_1]^+$ (X,Y = H,D or D,H) ($[\mathbf{C}_{M,R}^{\mathbf{X}}\cdot H\cdot N_1]^+/[\mathbf{C}_{P,S}^{\mathbf{Y}}\cdot H\cdot N_1]^+ = 1.15 \pm 0.12$; Fig. S1a). In contrast, the homochiral $[\mathbf{C}_{M,R}^{\mathbf{X}}\cdot H\cdot N_2]^+$ and the heterochiral $[\mathbf{C}_{P,S}^{\mathbf{Y}}\cdot H\cdot N_2]^+$ fragments arising from CID of $[\mathbf{C}_{M,R}^{\mathbf{X}}\cdot\mathbf{C}_{P,S}^{\mathbf{Y}}\cdot H\cdot N_2]^+$ (X,Y = H,D or D,H) exhibit a relative abundance significantly below unity ($([\mathbf{C}_{M,R}^{\mathbf{X}}\cdot H\cdot N_2]^+/[\mathbf{C}_{P,S}^{\mathbf{Y}}\cdot H\cdot N_2]^+ = 0.72 \pm 0.10$)[47] (Fig. S1b). This result is in full agreement with the more pronounced reactivity of the homochiral $[\mathbf{C}_{M,R}^{\mathbf{X}}\cdot H\cdot N_2]^+$ complexes, relative to that of the heterochiral $[\mathbf{C}_{P,S}^{\mathbf{Y}}\cdot H\cdot N_2]^+$ one, towards the same amine **B** in the FT-ICR experiments. The calculated relative energies of the $[\mathbf{C}'\cdot H\cdot N_1]^+$ diastereomeric adducts (Fig. 2; $\Delta E = E_{homo} - E_{hetero} = 0.12$ kcal mol^{-1}) are very close, whereas the corresponding values for $[\mathbf{C}'\cdot H\cdot N_2]^+$ differ more significantly ($\Delta E = 1.22$ kcal/mol).[48] This result apparently correlate well with the CID of $[\mathbf{C}_{M,R}^{\mathbf{X}}\cdot\mathbf{C}_{P,S}^{\mathbf{Y}}\cdot H\cdot N_1]^+$ and $[\mathbf{C}_{M,R}^{\mathbf{X}}\cdot\mathbf{C}_{P,S}^{\mathbf{Y}}\cdot H\cdot N_2]^+$. Therefore, the same stability of the diastereomeric $[\mathbf{C}\cdot H\cdot N_1]^+$ adducts indicates that the enantioselectivity values measured for this system mostly reflect the relative free Gibbs energy values of the corresponding transition structures. On the other hand, the combination of CID and kinetic results strongly supports the view that the enantioselectivity measured for the diastereomeric $[\mathbf{C}\cdot H\cdot N_2]^+$ adducts reflect either their relative stability as well as that of the transition structures involved across the reaction coordinate.

CONCLUSION

The interactions between a cyclochiral resorcin[4]arene and representative bidentate and tridentate guests have been explored in the gas phase. The results represent the first example of kinetic enantiodiscrimination exclusively due to the structural asymmetry of a macrocycle scaffold. Mostly, the heterochiral adducts react faster than their homochiral counterparts, with few exceptions ($\mathbf{G} = A_4$; N_2; N_4). In the most enantioselective system, the guest is an aromatic aminodiol, thus suggesting that basically, the guest does need two hydroxyl groups to selectively interact with the upper region of the chiral scaffold and one basic amino group to keep the charge and behave as the effective hook by sticking on the aromatic complex counterparts by cation–π interactions. This structural arrangement is confirmed by DFT calculations. The pronounced effect of the neutral gas proton affinity unambiguously indicates that the major enantioselectivity reason is the intimate interaction developed in the diastereomeric transition structures. This view is supported by CID of the three-body $[\mathbf{C}_{M,R}^{\mathbf{X}}\cdot\mathbf{C}_{P,S}^{\mathbf{Y}}\cdot H\cdot N_1]^+$ complexes that points to the same stability for diastereomeric $[\mathbf{C}_{M,R}^{\mathbf{X}}\cdot H\cdot N_1]^+$ and $[\mathbf{C}_{P,S}^{\mathbf{Y}}\cdot H\cdot N_1]^+$ complexes. Nevertheless, the CID result obtained for the $[\mathbf{C}_{M,R}^{\mathbf{X}}\cdot\mathbf{C}_{P,S}^{\mathbf{Y}}\cdot H\cdot N_2]^+$ adduct indicates the combination of thermodynamic and kinetic factors as the origin of the FT-ICR selectivity, the less stable homochiral species being even the more reactive one.

Acknowledgements

Dr. Heinrich Luftmann (Org. Chem. Inst. der Universität Münster) is gratefully acknowledged for the ESI-CID experiments. The financial support was provided by the Deutsche Forschungsgemeinschaft (SFB 613).

Supporting information

Supporting information may be found in the online version of this article.

REFERENCES

[1] F. Hollfelder, A. J. Kirby, D. S. Tawfik. Off-the-shelf proteins that rival tailor-made antibodies as catalysts. *Nature* **1996**, *383*, 60.
[2] J. A. Loo. Studying noncovalent protein complexes by electrospray ionization mass spectrometry. *Mass Spectrom. Rev.* **1997**, *16*, 1.
[3] J. A. Loo. Electrospray ionization mass spectrometry: a technology for studying noncovalent macromolecular complexes. *Int. J. Mass Spectrom.* **2000**, *200*, 175.
[4] A. J. Heck, R. H. H. Van den Heuvel. Investigation of intact protein complexes by mass spectrometry. *Mass Spectrom. Rev.* **2004**, *23*, 368.
[5] A. Filippi, N. Trout, A. P. Brunelle, W. Adcock, T. S. Sorensen, M. Speranza. Origin of diasterofacial selectivity in tertiary 2-adamantyl cations. *J. Am. Chem. Soc.* **2001**, *123*, 6396.
[6] A. Filippi, N. Trout, A. P. Brunelle, W. Adcock, T. S. Sorensen, M. Speranza. Importance of entropy in the diastereoslectivity of 5-substituted 2-methyladamant-2-yl cations. *J. Org. Chem.* **2004**, *69*, 5537.
[7] a) Y. Liang, J. S. Bradshaw, D. V. Dearden. The thermodynamic basis for enantiodiscrimination: gas-phase measurement of the enthalpy and entropy of chiral amine recognition by dimethyldiketopyridino-18-crown-6. *J. Phys. Chem. A* **2002**, *106*, 9665;
b) W. A. Tao, R. G. Cooks. Chiral analysis by MS. *Anal. Chem.*. **2003**, *75*, 25A and references therein.
[8] a) S. Starnes, D. M. Rudkevich, J. Rebek. Cavitand-porphyrins. *J. Am. Chem. Soc.* **2001**, *123*, 4659; b) U. Lücking, F. C. Tucci, D. M. Rudkevich,

J. Rebek. Self-folding cavitands od nanoscale dimensions. *J. Am. Chem. Soc.* **2000**, *122*, 8880; c) D. M. Rudkevich, J. Rebek. Depening cavitands. *J. Eur. Org. Chem.* **1999**, 1991; d) D. M. Rudkevich. Nanoscale molecular containers. *Bull. Chem. Soc. Jpn.* **2002**, *75*, 393.

[9] D. J. Cram, J. M. Cram. Container Molecules and Their Guests. The Royal Society of Chemistry: Cambridge; **1994**.

[10] a) T. Heinz, D. M. Rudkevich, J. Rebek. Pairwise selection of guests in a cylindrical molecular capsule of nanometre dimension. *J. Nature* **1998**, *394*, 764; b) D. M. Rudkevich. *Calixarenes* **2001**; c) Z. Asfari, V. Böhmer, J. Harrowfield, J. Vicens (Eds). Kluwer: Dordrecht The Netherlands. **2001**, 155; (d) F. Hof, S. L. Craig, C. Nuckolls, J. Rebek. Molecular encapsulation. *Angew. Chem. Int. Ed.* **2002**, *41*, 1488.

[11] C. Reuter, R. Schmieder, F. Vögtle. From rotaxanes to knots. Templating, hydrogen bond patterns, and cyclochirality. *Pure Appl. Chem.* **2000**, *12*, 2233.

[12] A. Szumna. Cyclochiral conformers of resorcin[4]arenes stabilized by hydrogen bonds. *Org. Biomol. Chem.* **2007**, *5*, 1358.

[13] a) A. Dalla Cort, C. Mandolini, L. Pasquini, L. Schiaffino. "Inherent chirality" and curvature. *New J. Chem.* **2004**, *28*, 1198; b) Y. S. Zheng, J. Luo. Inherently chiral calixarenes: a decade's review. *J. Incl. Phenom. Macrocycl. Chem.* **2011**, DOI 10.1007/s10847-011-9935-4.

[14] M. Vincenti, A. Irico. Gas-phase interactions of calixarene and resorcinarene cavitands with molecular guests studied by mass spectrometry. *Int. J. Mass Spectrom.* **2002**, *214*, 23 and references therein.

[15] M. W. Makinen, P. Vainiotalo, M. Nissinen, K. Rissanen. Ammonium ion mediated resorcarene capsules: ESI-FT-ICRMS study on gas-phase structure and ammonium ion affinity of tetraethyl resorcarene and its per-methylated derivative. *J. Am. Soc. Mass Spectrom.* **2003**, *14*, 143.

[16] M. W. Makinen, P. Vainiotalo, K. Rissanen. Alkali metal mediated resorcarene capsules: an ESI-FTICRMS study on gas-phase structure and cation binding of tetraethyl resorcarene and its per-methylated derivative. *J. Am. Soc. Mass Spectrom.* **2002**, *13*, 851.

[17] M. Vincenti, A. Irico, E. Dalcanale. *Adv. Mass Spectrom.* **1998**, 14, Chaps. 7/129 7/150, and references therein.

[18] M. Vincenti, E. Dalcanale. Host–guest complexation in the gas phase. Investigation of the mechanism of interaction between cavitands and neutral guest molecules. *J. Chem. Soc. Perkin Trans.* **1995**, *2*, 1069.

[19] B. Botta, I. D'Acquarica, L. Nevola, F. Sacco, Z. V. Lopez, G. Zappia, C. Fraschetti, M. Speranza, A. Tafi, F. Caporuscio, M. C. Letzel, J. Mattay. Bis(diamido)-bridged basket resorcin[4]arenes as enantioselective receptors for amino acids and amines. *Eur.J. Org. Chem.* **2007**, 5995, and the references therein.

[20] B. Botta, A. Tafi, F. Caporuscio, M. Botta, L. Nevola, I. D'Acquarica, C. Fraschetti, M. Speranza. Modelling amphetamine/receptor interactions: a gas-phase study of complexes formed between amphetamine and some chiral amido[4]resorcinarenes. *Chem. Eur. J.* **2008**, *14*, 3585.

[21] B. Botta, C. Fraschetti, F. R. Novara, A. Tafi, F. Sacco, L. Mannina, A. P. Sobolev, J. Mattay, M. C. Letzel, M. Speranza. Interactions of vinca alkaloids with chiral amido[4]resorcinarenes: a dynamic, kinetic, and spectroscopic study. *Org. Biomol. Chem.* **2009**, *7*, 1798, and the references therein.

[22] B. Botta, C. Fraschetti, I. D'Acquarica, M. Speranza, F. R. Novara, J. Mattay, M. C. Letzel. Gas-phase enantioselectivity of chiarl *N*-linked peptidoresorc[4]arene isomers toward dipeptides. *J. Phys. Chem. A* **2009**, *113*, 14625, and the references therein.

[23] A. Mehdizadeh, M. C. Letzel, M. Klaes, C. Agena, J. Mattay. Chiral discrimination on the host-guest-complexation of resorc[4]arenes with quarternary amines. *Eur. J. Mass Spectrom.* **2004**, *10*, 649.

[24] R. Buckley, J. Y. Boxhall, P. C. Bulman Page, Y. Chan, M. R. J. Elsegood, H. Heaney, K. E. Holmes, M. J. McIldowie, V. McKie, M. J. McGrath, M. Mocerino, A. M. Poulton, E. P. Sampler, B. W. Skelton, A. H. White. Mannich and O-alkylation reactions of tetraalkoxyresorcin[4]arenes – the use of some products in ligand-assisted reactions. *Eur. J. Org. Chem.* **2006**, *22*, 5117.

[25] M. J. McIldowie, M. Mocerino, B. W. Skelton, A. H. White. Facile Lewis acid catalyzed synthesis of C_4 symmetric resorcinarenes. *Org. Lett.* **2000**, *24*, 3869.

[26] C. Schiel, G. A. Hembury,V. V. Borovkov, M. Klaes, C. Agena, T. Wada, S. Grimme, Y. Inoue, J. Mattay. New insight into the geometry of resorc[4]arenes: solvent-mediated supramolecular conformational and chiroptical control. *J. Org. Chem.* **2006**, *71*, 976.

[27] M. Gangoda, R. K. Gilpin, J. Figueirinhas. Deiterium nuclear magnetic resonance studies of alkyl-modified silica. *J. Phys. Chem.* **1989**, *93*, 4815.

[28] M. Sawada. Chiral recognition in host-guest complexation determined by FAB mass spectrometry. *J. Mass Spectrom. Soc. Jpn.* **1997**, *45*(3), 439.

[29] X. Quin, T. Tzvetkov, X. Liu, D. C. Lee, L. Yu, D. C. Jacobs. Site-selective abstraction in the reaction of 5–20 eV O^+ with a self-assembled monolayer. *J. Am. Chem. Soc.* **2004**, *126*, 13232.

[30] J. Terao, H. Todo, S. A. Begum, H. Kuniyasu, N. Kambe. Copper-Catalyzed cross-coupling reaction of grignard reagents with primary-alkyl halides: remarkable effect of 1-phenylpropyne. *Angew. Chem. Int. Ed.* **2007**, *46*, 2086.

[31] M. Gaddis, R. Ellis, G. T. Currie. Girard *T* Reagent for Carbonyls. *Nature* **1961**, *191*, 1391.

[32] M. Klaes, C. Agena, M. Köhler, M. Inoue, T. Wada, Y. Inoue, J. Mattay. First synthesis, isolation and characterization of enantiomerically pure and inherently chiral resorc[4]arenes by Lewis acid cyclization of a resorcinol monoalkyl ether. *Eur. J. Org. Chem.* **2003**, *8*, 1404.

[33] R. Buckley, P. C. Bulman Page, Y. Chan, H. Heaney, M. Klaes, M. J. McIldowie, V. McKee, J. Mattay, M. Mocerino, E. Moreno, B. W. Skelton, A. H. White. The preparation and absolute configurations of enantiomerically pure C_4-symmetric tetraalkoxyresorcin[4]arenes obtained from camphorsulfonate derivatives. *Eur. J. Org. Chem.* **2006**, *22*, 5135.

[34] R. Ahlrichs, M. Baer, M. Haeser, H. Horn, C. Koelmel. Electronic structure calculations on workstation computers: the program system turbomole. *Chem. Phys. Lett.* **1989**, *162*, 165.

[35] A. D. Becke. Density-functional exchange-energy approximation with correct asymptotic behavior. *Phys. Rev. A* **1988**, *38*, 3098.

[36] J. P. Perdew. Density-functional approximation for the correlation energy of the inhomogeneous electron gas. *Phys. Rev. B.* **1986**, *33*, 8822.

[37] a) B. I. Dunlap, J. W. Conolly, J. R. Sabin. On some approximations in applications of $X\alpha$ theory. *J. Chem. Phys.* **1979**, *71*, 3396; b) O. Vahtras, J. Almlöf, M. W. Feyereisen. Integral approximations for LCAO-SCF calculations. *Chem. Phys. Lett.* **1993**, *213*, 514; K. Eichkorn, O. Treutler, H. Öhm, M. Häser, R. Ahlichs. Auxiliary basis sets to approximate Coulomb potentials. *Chem. Phys. Lett.* **1995**, *240*, 283.

[38] K. Eichkorn, O. Treutler, H. Ohm, M. Haser, R. Ahlrichs. Auxiliary basis sets to approximate Coulomb potentials. *Chem. Phys. Lett.* **1995**, *242*, 652; R. Ahlrichs, M. Arnim. Methods and Techniques in Computational Chemistry, MET ECC-95 (ed.) E. Clementi, G. Corongiu, STEF: Cagliari; **1995**, 509.

[39] A. Schaefer, C. Huber, R. Ahlrichs. Fully optimized contracted Gaussian basis sets of triple zeta valence quality for atoms Li to Kr. *J. Chem. Phys.* **1994**, *100*, 5829.

[40] S. Grimme. Semiempirical GGA-Type Density functional constructed with a long-range dispersion correction. *J. Comput. Chem.* **2006**, *27*, 1787.

[41] S. Grimme, J. Antony, T. Schwabe, C Mück-Lichtenfeld. Density functional theory with dispersion corrections for supramolecular structures, aggregates, and complexes of (bio)organic molecules. *Org. Biomol. Chem.* **2007**, *5*, 741.

[42] P. Deglmann, K. May, F. Furche, R. Ahlrichs. Nuclear second analytical derivative calculations using auxiliary basis set expansions. *Chem. Phys. Lett.* **2004**, *384*, 103; P. Deglmann, K. May, F. Furche, R. Ahlrichs. An efficient implementation of second analytical derivatives for density functional methods. *Chem. Phys. Lett.* **2002**, *362*, 511; P. Deglmann, K. May, F. Furche. Efficient characterization of stationary points on potential energy surfaces. *J. Chem. Phys.* **2002**, *117*, 9535.

[43] VMD for WIN-32, Version 1.8.3 (Februar, 15, 2005); see also W. Humpfrey, A. Dalke, K. Schulten. VMD: visual molecular dynamics. *J. Mol. Graphics.* **1996**, *14*, 33.

[44] a)T. Su, W. J. Chesnavitch. Parametrization of the ion–polar molecule collision rate constant by trajectory calculations. *J. Chem. Phys.* **1982**, *76*(10), 5183; b) T. Su. Erratum: trajectory calculations of ion-polar molecule capture rate constants at low temperatures [J. Chem. Phys. 1988, 88, 4102]. *J. Chem. Phys.* **1988**, *89*(8), 5355.

[45] Kinetic isotope effect expressed as k_H/k_D.

[46] The used gas phase basicities have been taken from the http://webbook.nist.gov/chemistry/ site.

[47] For instance $\Delta PA = PA_{ethanolamine}\text{-}PA_{glycine} = 10.4$ kcal mol^{-1} (http://webbook.nist.gov/chemistry/) and $\Delta PA = PA_{methyl\ ester}\text{-}PA_{glycine} = 3.8$ kcal mol^{-1} (M. J. Locke, R. T. McIver Jr. Effect of solvation on the acid/base properties of glycine. *J. Am. Chem. Soc.* **1983**, *105*, 4226).

[48] The diastereomeric excess found for $[\mathbf{C}_{P,S}^{\mathbf{Y}}\cdot H\cdot N_2]^+$ adduct corresponds to the relative free energy difference of only approximately 0.2 kcal mol^{-1}.